

Research Article

RECOGNITION DYNAMICS OF *ESCHERICHIA COLI* THIOREDOXIN PROBED USING MOLECULAR DYNAMICS AND BINDING FREE ENERGY CALCULATIONS

M. S. Shahul Hameed

Department of Biotechnology, Bannari Amman Institute of Technology, Sathyamangalam- 638401, Erode District Tamil Nadu, India

Abstract: *E. coli* thioredoxin has been regarded as a hub protein as it interacts with, and regulates, numerous target proteins involved in a wide variety of cellular processes. Thioredoxin can form complexes with a variety of target proteins with a wide range of affinity, using a consensus binding surface. In this study an attempt to deduce the molecular basis for the observed multispecificity of *E. coli* thioredoxin has been made. In this manuscript it has been shown that structural plasticity, adaptable and exposed hydrophobic binding surface, surface electrostatics, closely clustered multiple hot spot residues and conformational changes brought about by the redox status of the protein have been shown to account for the observed multispecificity and molecular recognition of thioredoxin. Dynamical differences between the two redox forms of the enzyme have also been studied to account for their differing interactions with some target proteins.

Key Words: Thioredoxin; protein-protein interaction; multispecificity; conformation selection model; binding hot spots; correlated motions.

Coloured figures and supplementary available on journal website

Introduction

Molecular recognition by proteins is essential to almost every physiological process such as signaling, catalysis, gene regulation etc. The most important elements of molecular recognition are specificity and affinity. The ability to form non-covalent complexes of high affinity and specificity is a fundamental property of biological macromolecules. However affinity and specificity, though different concepts, are negatively correlated in certain cases. A considerable number of proteins have evolved to bind multiple targets, including other proteins, peptides and small molecules. Such proteins with

diverse binding capacity have been termed multispecific proteins. Increasing evidence for multispecificity in protein-protein interactions is accumulating and several proteins play a highly important role in the cell as they bind to and regulate a large number of partners (Erijman *et al.*, 2011). Multispecific proteins are often termed as hub proteins as they represent highly connected nodes in protein interaction networks (Tsai *et al.*, 2009). Deletion mutations involving hubs are often lethal to the organism as the entire protein interaction network topology may be affected (Jeong *et al.*, 2001). Therefore hub proteins constitute novel targets for designed pharmaceutical drugs. Multispecificity may be achieved either by having a distinct binding interface for each target protein (e.g. multidomain proteins) or utilizing the same or highly overlapping binding interface for binding multiple partners (single interface hubs). It would

Corresponding Author: M. S. Shahul Hameed
E-mail: shahulhambiotech@gmail.com

Received: August 25, 2015

Accepted: January 17, 2016

Published: January 20, 2016

be interesting to know how a single binding surface has evolved to bind multiple targets that differ in sequence and 3D structure.

Proteins like calmodulin, p53, p21, p27, Ras, thioredoxin and ubiquitin are some of the well established single interface hub proteins. Thioredoxins from different organisms show a sequence identity of 27 - 69% to *E. coli* thioredoxin. Thioredoxin acts as a hub protein in an extensively coupled network of redox regulation. Proteomic studies of Thioredoxin (Trx) targeted proteins in *E. coli* have identified atleast 80 different proteins associated with Trx, belonging to at least 26 distinct cellular processes including energy metabolism, cell division, detoxification, oxidative stress response, transport, small molecule biosynthesis and degradation, DNA replication and recombination, protein translation, protein modification and protein degradation (Kumar *et al.*, 2004). Thioredoxin plays a protective role by preventing the aggregation/inactivation, via oxidative formation, of cytosolic proteins. Thioredoxins with a dithiol/disulfide active site are the major cellular protein disulfide reductases and serve as electron donors for ribonucleotide reductase, PAPS reductase, peroxiredoxins, methionine sulfoxide reductase and DsbD (Arner and Holmgren 2000). Thioredoxins are involved in redox signaling as they catalyse thiol-disulfide exchange reactions, which are rapid, readily reversible and ideally suited to control protein function (Fujino *et al.*, 2006). Apart from regulating target proteins through its oxidoreductase activity, thioredoxin regulates a wide variety of proteins through a mechanism which does not involve thiol redox activity. Such regulation depends on the ability of thioredoxin to form functional protein complexes by exacting protein-protein interactions as these thioredoxin linked proteins do not contain regulatory cysteines. The most striking example of such thioredoxin targets is T7 DNA polymerase, where reduced Trx is involved in a high affinity interaction with it and confers high processivity on the enzyme (Huber *et al.*, 1987). Reduced Trx takes part in phage assembly by forming complexes with filamentous phage proteins (Russel and Model, 1986). It has been shown that mammalian thioredoxin forms inhibitory

complexes with apoptosis signaling kinase I (Saitoh *et al.*, 1998).

The binding surface of thioredoxin which is flat and hydrophobic is highly conserved across species and overlaps with members of the glutaredoxin family (Eklund *et al.*, 1984). In addition to the active site sequence Cys32-Gly33-Pro34-Cys35, a number of other residues involved in binding interactions with target proteins are highly conserved. They include Trp31, Lys36, Met37, Lys57, Asp61, Pro64, Arg73, Ile75, Val91, Gly92, Ala93 and Lys96 (Eklund *et al.*, 1991). It has been shown that the amount of charge polarization around the active site surface of Trx influences the specificity of its interaction with target proteins. *E.coli* thioredoxin with less polarization around the active site compared to mitochondrial thioredoxins shows higher cross reactivity (Raddatz *et al.*, 2000). In this study the molecular basis behind the observed multi-specificity of *E.coli* thioredoxin in binding partner proteins has been addressed. Interface analysis of known complexes of thioredoxin has revealed the hot spot residues which are present in the conserved binding surface of Trx. MD simulations captured the changing surface area of the conserved surface patches and provides an explanation of the adaptive plasticity of Trx associated with its multi-specificity. The electrostatic contributions to binding have been deduced by calculating electrostatic potential surface maps and dipole moment. The role of Arg73 as an anchor residue has been probed. Furthermore the observed differences in binding between the two redox forms of thioredoxin have also been studied.

Materials and Methods

Interface analysis

Protein Interface analysis were carried out using PROFACE (Saha *et al.*, 2006) and PROTORG (Reynolds *et al.*, 2009) web-servers.

Molecular dynamics

Molecular dynamics (MD) simulations were carried out using the AMBER suite of programs (version- AMBER 9) (Case *et al.*, 2006) with the ff99 force field parameters. The simulations were

carried out for atleast 50ns for both the reduced and oxidized forms of *E. coli* thioredoxin. The starting conformations for the MD simulations for oxidized and reduced forms of Trx were taken from structure files PDB ID: 1xoA and PDB ID: 1xob (Jeng *et al.*, 1994) respectively. For all the simulations periodic truncated octahedron box was used for solvation of the protein in explicit TIP3P water molecules. The molecular systems were neutralized with Na⁺ ions. The initial solvated structures were first subjected to 200 steps steepest descent energy minimization, whereas the solute atoms, including the protein, were restrained by a harmonic potential with a force constant of 100.0 kcal/mol/Å². After the initial solvent minimization, the whole system was minimized using 200 steps of steepest descent minimization without harmonic restraints. The minimized structures were then subjected to an equilibration protocol in which the temperature of the systems were gradually raised from 100K to 300K over a 10ps period while holding both the volume and temperature constant, followed by another 10ps at 300K by holding the temperature and pressure constant while allowing the volume to change for adjusting solvent density. The initial velocities were randomly assigned from a Maxwellian distribution at 100K. At the end of the equilibration, the average temperature was 300K, and the average density was 1.0 g/ml. Long range electrostatic interactions were treated with the particle mesh Ewald method. Periodic boundary conditions were applied via both nearest image and the discrete Fourier transform implemented as part of the particle mesh Ewald method. All bonds involving hydrogen atoms were restrained using the SHAKE algorithm with time steps of 2fs to be taken. Global translation and rotation of the system (solvent and solute) was removed every 100 integration steps during the simulation. The initial 20ps stage was designed to equilibrate those particles that were added during the initial model-building process, including water molecules and hydrogen atoms, and to allow the systems to be solvated adequately. The initial 20ps trajectories were discarded and were followed by the production stage in which both pressure (1.0 atm) and temperature (300K) were held constant by Berendsen's coupling scheme. The essential

dynamics of the two forms of thioredoxin was extracted from the MD simulation trajectories by using PCA analysis of the covariance matrices using PTRAJ (amber 9) and Gromacs utilities (Hess *et al.*, 2008). The fluctuation contributions from translational and rotational motions of the protein were removed by aligning each snapshot onto the initial conformation. Only C^a atom coordinates were used for constructing the covariance matrices. Interactive Essential Dynamics coupled with VMD was used to visualize the top Eigen mode motions (Mongan *et al.*, 2004). To estimate the difference in conformational entropies between the bound and unbound forms of thioredoxin, we have performed quasi-harmonic entropy calculations (Karplus *et al.*, 1981). This involved diagonalization of the mass-weighted covariance matrix describing average backbone atom fluctuations from trajectories of the systems with overall translations and rotations removed.

Cross-Correlation analyses

The dynamic characteristics of the enzyme in the simulations can be analyzed to yield information about correlated motions. Cross correlation maps are used to identify the regions, which move in or out of phase during the simulations. Correlated displacements of protein residue/atom during the simulation can be described by equation 1 (Hunenberger *et al.*, 1995).

$$C_{ij} = \frac{<(r_i - <r_i>)(r_j - <r_j>)>}{\sqrt{(<r_i^2> - <r_i>^2)(<r_j^2> - <r_j>^2)}} \quad (1)$$

where i and j may correspond to any two atoms, residues or domains. r_i and r_j are position vectors of i and j, and the angle brackets denote an ensemble average. Inter-atomic cross-correlation fluctuations between any two pairs of atoms (or residues) were calculated using this expression and represented graphically by the dynamic cross correlation map (DCCM) using MATLAB 7.5. The value of C_{ij} can vary from -1 (completely anti-correlated motion) to +1 (completely correlated motion).

Helix analysis

The program TRAJELIX from Simulaid suite of programs (Mezei *et al.*, 2010) was used to analyze

the changes of important helical properties like helix tilt, helix angle, helix displacement, residues per turn along the ten nanoseconds molecular dynamics run. PRO-KINK (Simulaid) was used to analyze the changes in bend angle about Pro40 residue, along the 10ns molecular dynamics run for both the forms of the protein.

Binding free energy calculations

Free Energy calculations were carried out for the three systems using the MM/PBSA method (Kollman *et al.*, 2000).

The binding free energy was calculated as:

$$\begin{aligned}\Delta\Delta G_{\text{bind}} &= \Delta G_{\text{complex}} - \Delta G_{\text{target-protein}} - \Delta G_{\text{Trx}} \\ &= \Delta E_{\text{MM}} + \Delta G_{\text{PB}} + \Delta G_{\text{SA}} - T\Delta S\end{aligned}$$

where ΔE_{MM} is the molecular mechanics interaction energy between thioredoxin and its binding partner. ΔG_{PB} and ΔG_{SA} are the electrostatic and non-polar contributions to desolvation upon binding respectively, and $-T\Delta S$ is the conformational entropy change. To consider the conformational flexibility of the proteins, separate set of MD simulations on the complexes and the free proteins were run to calculate the binding free energy. MD simulations were carried out for atleast 20ns for T7pol-Trx complex (PDB ID: 1t7p), TrxR-Trx complex (PDB ID: 1f6m, only the A chain and C chain were used) and Bt-Trx complex (PDB ID: 2bto, only the A chain and T chain were used) (Doublet *et al.*, 1998; Lennon *et al.*, 2000; Schlieper *et al.*, 2005). The starting structures for the unbound conformations of T7pol, TrxR and Bt were generated after removing other chains from the structure files PDB ID: 1t7p, PDB ID: 1f6m and PDB ID: 2bto respectively followed by extensive minimization for atleast 500 steps of steepest descent minimization. MD simulations for T7pol, TrxR and Bt were carried out for 20ns. For all the simulations, equilibration was carried out for a total of 1ns before the production run.

ΔE_{MM} was calculated using the sander program in AMBER 9. ΔG_{PB} was calculated using the PBSA program in AMBER 9. The grid size used to solve the Poisson-Boltzmann equation was 0.5 Å, and the values of interior dielectric constant and exterior dielectric constant were set to 1 and 80, respectively. ΔG_{SA} was estimated from

the surface area. The interaction energies were calculated from 150 snapshots taken from 10ns to 20ns MD simulation trajectories of the complex. 150 snapshots taken from 10ns to 20ns MD simulations on the free proteins were used to calculate the conformational energy change for the proteins.

The normal mode analysis was performed to estimate the vibrational component of the entropy using the nmode program in AMBER 9. In the absence of solvent, the structures (complex, target proteins, and thioredoxin) were minimized by using conjugate gradient and then Newton-Raphson minimizations until the root mean square of the elements of gradient vector was less than 5×10^{-5} Kcal/mol. A distance-dependent dielectric constant was used to mimic solvent screening. Frequencies of the vibrational modes were computed at 300K for these minimized structures and using a harmonic approximation of the energies. Due to the high computational demand, only 50 snapshots taken from MD were used to estimate conformational entropy ($-T\Delta S$). The binding free energy was then decomposed into residue-wise and pair-wise contributions across the interface.

Interface Cluster Analysis

Interface cluster analysis was done using the molecular dynamics analysis package Wordom (Seeber *et al.*, 2007).

Results

Interface analysis

The three thioredoxin complexes used in this study are T7pol-Trx complex – a high affinity complex ($K_d \sim 3\text{nM}$) between reduced thioredoxin and gene5 protein of bacteriophage T7, TrxR-Trx complex – a complex between thioredoxin (Trx) and thioredoxin reductase (TrxR) stabilized through a mixed disulfide, and a non-specific complex between thioredoxin (used as a tag) and bacterial tubulin (Bt) from Prosthecobacter de Jongeii. Interface analysis of known complexes of *E. coli* thioredoxin reveals the fact that thioredoxin uses a highly similar binding surface for interacting with a range of target proteins differing both in structure and

sequence. Gap Volume Index varies significantly among the three thioredoxin complexes. The nonspecific complex Bt-Trx shows high GI values while specific complexes T7pol-Trx and TrxR-Trx show low values. The planarity of the complex, which is a measure of shape complementarity, also seems to vary among the different thioredoxin complexes with nonspecific Bt-Trx complex showing the lowest value (Table 1). The thioredoxin binding surface of T7 DNA polymerase was found to contain only loop regions while in the other two complexes it involved mostly loops apart from other secondary structural components. Structural analysis of these complexes shows that thioredoxin uses almost the same set of contact residues for binding many proteins. Analysis of the consensus binding surface revealed that it was distinguished by a high degree of solvent accessibility and a predominantly non-polar character, suggesting that burial of exposed hydrophobic surface area is an important driving force behind binding at this site. The hydrophobic patch around the active site of thioredoxin constituted by residues Trp31, Cys32, Gly33 and Pro34 takes part in all known protein-protein interactions of Trx with various partner proteins. Similarly residues in the flexible

loop connecting helix-3 to β sheet-4 (Gly71, Ile72, Arg73, Gly74 and Ile75) and the one connecting β sheet-5 to the C-terminal helix (Val91, Gly92, Ala93 and Leu94) and residues in exposed surface of helix-3 (Ile60, Asp61, Pro64, Ala67 and Pro68) are also involved in protein-protein interactions with target proteins. In all three complexes it was found that sidechains of Trx residues Trp³¹ and Arg⁷³ contribute significantly to the interface accessible surface area. Trp³¹ provides 11.6%, 8.3% and 20% of interface accessible surface area in T7pol-Trx, TrxR-Trx and Bt-Trx complexes, respectively while Arg⁷³ provides 10.63%, 21.02% and 18.34% of interface accessible surface area in T7pol-Trx, TrxR-Trx and Bt-Trx complexes, respectively.

The spatially conserved chemical interactions shared by thioredoxin binding interfaces of T7 DNA polymerase, Thioredoxin reductase and B-tubulin complexes were identified using multiple alignment of protein-protein complexes. Only few spatially conserved interactions were identified which include aliphatic interactions with Pro34 and Cys32 residues of thioredoxin and hydrogen bonding interactions with the backbone atoms of the highly conserved Ile75 of thioredoxin.

Table 1
Interface characteristics of Thioredoxin complexes

a

Partner proteins	Trx residues	Total IASA (\AA^2)	IASA of Trx (\AA^2)
T7 DNA polymerase	E30, W31, C32, G33, P34, K36,M37, I60, D61, P64, A67, P68, I72, R73, G74, I75, T89, K90, V91, G92, A93, L94 and Q98	1866 \AA^2	900 \AA^2
Thioredoxin reductase	W31, C32, G33, P34, M37, P40,I41, E44, I60, P64, A67, Y70, G71, I72, R73, G74, I75, V91, A93, L94, S95, K96, G97 and Q98	1805 \AA^2	910 \AA^2
Tubulin	W31, C32, P34, M37, I60, D61, P64, A67, P68, G71, I72, R73, G74, I75, V91,G92 and A93	1200 \AA^2	575.66

b

Target proteins	% polar residues		% Non-polar residues		Charged residues		S.S ^a	P ^b	GI ^c
	Partner	Trx	Partner	Trx	Partner	Trx			
T7 DNA pol	34.78	17.39	52.17	60.87	13.04	21.74	Coil	2.898	1.96
Trx reductase	40.74	22.22	37.04	62.96	22.22	14.81	Coil/á	3.367	3.23
Btuba (A chain)	33.33	11.11	61.11	77.78	5.56	11.11	á	1.984	4.47

^aSecondary structure, ^bPlanarity, ^cGap Volume Index

Electrostatic interactions

The binding surface of thioredoxin possesses charged residues like Glu30, Lys36, Glu44, Asp61, Arg73, Lys90 and Lys96 at its periphery. The surface electrostatic potential maps computed using APBS for different conformations of *E.coli* thioredoxin are shown in Figure 1. In the TrxR-Trx complex 14 salt bridges were identified while 3 and 4 salt bridges were identified across the

protein-protein interface for T7pol-Trx complex and the Bt-Trx complex respectively. Arg73 contributes the maximum number of intermolecular hydrogen bonds with target proteins in all the analyzed *E. coli* Trx complexes. Thioredoxins across species are generally found to have polar residues at position 73 (*E. coli* numbering). Arginine at position 73 is unique to *E.coli* and is replaced by Lys at this position in

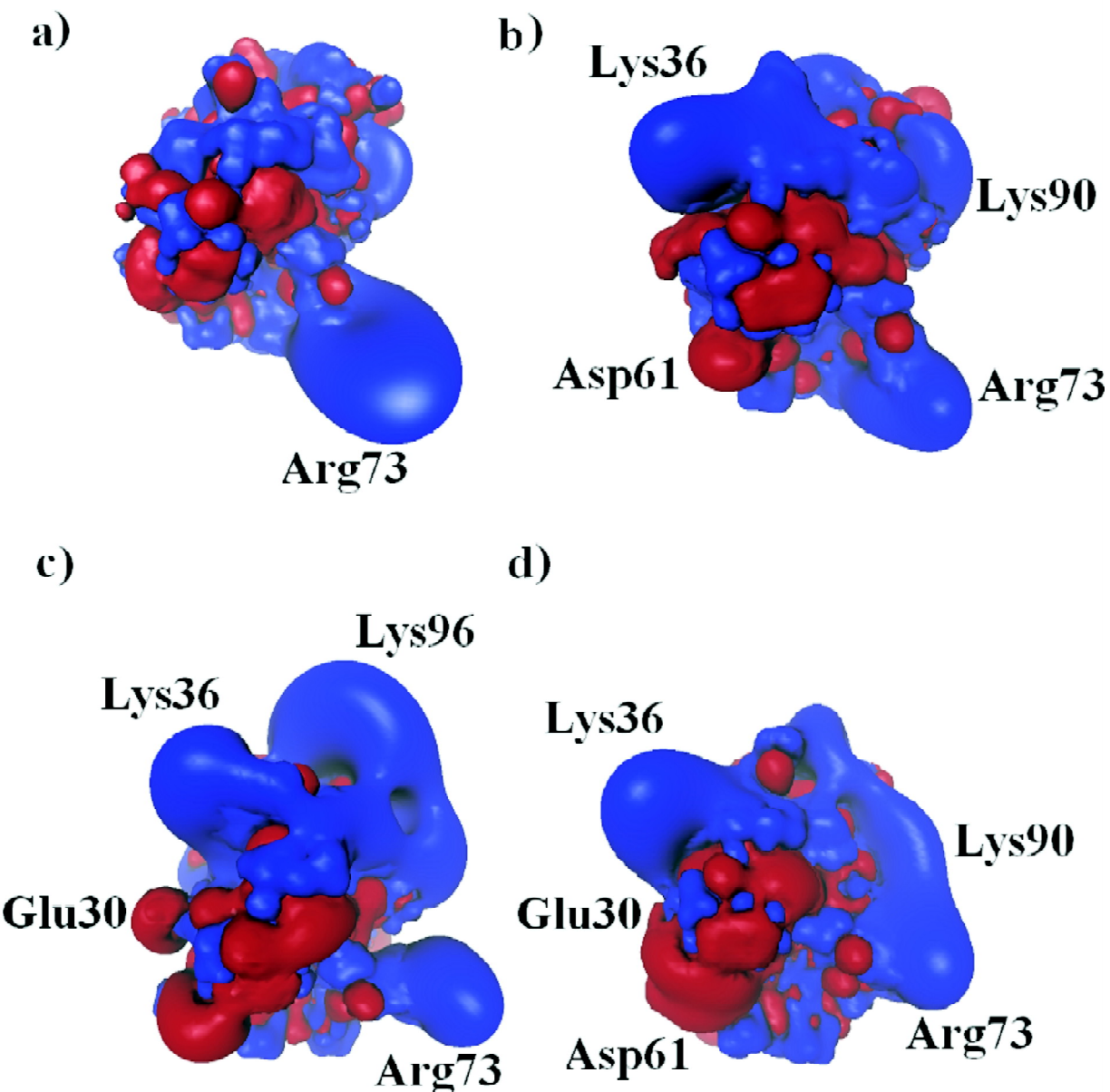


Figure 1: Electrostatics potential plots for different conformations of *E.coli* thioredoxin.

- Bound conformation of *E.coli* thioredoxin from Thioredoxin reductase thioredoxin complex.
- Bound conformation of *E.coli* thioredoxin from T7Polymerase thioredoxin complex.
- Unbound conformation of *E.coli* thioredoxin (PDB ID: 1XOB)

Human Trx. The side-chain dynamics were analyzed by extracting snapshots from each MD trajectory and overlapping them with the bound protein structure. It was found that some of the snapshots adopted conformations of Arg73 similar to that of the bound form. The role of loop residue Arg73 of *E. coli* Trx in its binding interaction with TrxR may serve as an anchor residue (**Supplementary Figure 1**). Interface accessible surface area of Arg73 in all the three bound complexes was high which accounts for ~20.5% of the interface. Arg73 contributes significantly to the binding free energy (~7 Kcal/mol) mostly because of favourable electrostatic interactions. It interacts very strongly with Ala237, Arg130, Gly129, Phe142 residues of TrxR. Other residues like Trp31, Ile72, Ile75 and Ala93 were also found to be frequently involved in hydrogen bond formation with target proteins across the interface.

Dipole moment of Trx

The dipole moment calculated for the bound conformation of thioredoxin in TrxR-Trx complex and Bt-Trx complex was found to be 280 debyes. The bound conformation of reduced Trx in T7pol-Trx complex had a dipole moment of 310 debyes in T7pol-Trx complex. The dipole moment computed for reduced thioredoxin (unbound conformation) was found to be ~ 375–410 debyes. During the course of simulations it was found that,

apart from moderate changes in the magnitude of dipole moment, the direction of the dipole moment varied considerably and some representative snapshots have been shown in Figure 2.

Geometric organization of hot spot residues

To get a better insight into molecular recognition of protein surfaces, it is important to obtain the quantitative contributions of the individual forces governing binding affinity and specificity. In this study, MM-PBSA approach was used to identify the critical residues playing an energetically important role in complex formation. Based on the contributions of residues to the binding free energy difference, the residues in the binding surface of Trx having significance in binding were identified (Table 2). The residues in the Trx and in the partner proteins which have a contribution of more than 2Kcal/mol to the enthalpic contributions to the total binding free energy difference were defined as hot spots. Residues in Trx, viz., Trp31, Tyr70, Arg73, Ile75, Val91 and Lys96 have been identified as hot spot residues from the present analysis of known Trx-target complexes (Table 2). Pairwise decomposition of binding free energy of Trx complexes helps us to understand the specificity and affinity components of protein-protein interactions of thioredoxin (Table 3).

Residues Trp31, Cys32, Pro34, Ile60, Ile72, Gly74, Ile75 and Ala93 contribute significantly to

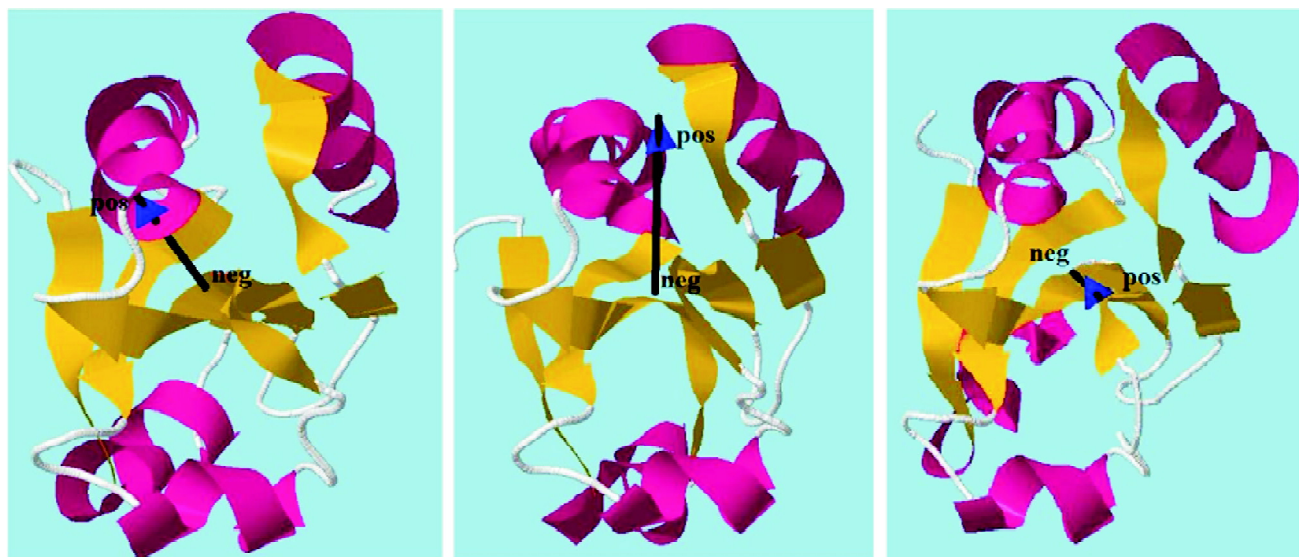


Figure 2: Dipole moments of some snapshot conformations from the 50ns MD trajectory

Table 2
Residue wise decomposition of binding free energy for Trx complexes

Res	T7P-Trx				TrxR-Trx				Btuba-Trx			
	IASA	Δ_{desol}	Δ_{ele}	Δ_{bind}	IASA	Δ_{desol}	Δ_{ele}	Δ_{bind}	IASA	Δ_{desol}	Δ_{ele}	Δ_{bind}
31W	106.51	-2.830	-0.161	-2.992	74.60	-2.085	-0.399	-2.484	114.86	-0.967	-0.842	-1.809
32C	16.43	-1.511		-1.467	21.40	-1.751	-0.192	-1.942	7.75	-1.173	-	-1.149
33G	46.44	-0.703		-0.698	14.36	-0.279	-0.329	-0.608	1.19	-0.089		-0.040
34P	57.30	-1.843		-1.808	31.35	-0.566	-0.112	-0.678	44.36	-0.863	-	-0.887
36K		0.834	3.408	4.242	-	-	-0.461	-	7.37			0.395
37M	58.95	-1.137	-	-1.192	89.95	-1.264	-0.126	-1.390	-	-	-	-
41I	-	-	-	-	17.20	-0.725	0.050	-0.675	-	-	-	-
44E	-	-	-	-	33.45	1.270	2.165	3.435	-	-	-	-
60I	32.68	-1.173	-	-1.192	29.53	-1.065	-0.049	-1.114	32.18	-1.082	-	-1.098
61D	11.65	0.287	-	-0.454		-0.062	0.214	0.152	4.62	0.164	-	0.079
64P	45.98	-0.373	-	-0.286	6.71	-0.050	-	-	36.68	0.122	0.571	0.693
67A	8.28	-0.288	-	-0.581	5.27	-0.067	-	-	8.32	-0.435	-	-0.462
68P	47.57	-0.448	-	-0.373	2.50	-	-	-	40.68	-0.920	-	-0.821
70Y	-	-	-	-	21.01	0.265	-2.501	-2.236	-	-	-	-
71G	-	-	-	-	47.69	0.206	-0.289	-	22.83	-0.139	-0.191	-0.330
72I	30.91	-1.036	-0.419	-1.455	18.86	-0.506	-0.379	-0.885	31.34	-0.863	-0.476	-1.339
73R	97.90	0.642	-1.167	-0.524	189.64	1.141	-9.008	-7.867	105.6	0.057	0.565	0.622
74G	23.29	-0.650	-0.125	-0.776	29.78		-1.082	-1.108	27.4	-0.571	-0.143	-0.714
75I	31.83	-1.899	-1.302	-3.202	30.82	-1.222	-0.451	-1.673	35.31	-2.083	-1.130	-3.213
90K	46.16	1.434	-2.052	-0.619	-	-	-1.088	-1.088	-	-	-	-
91V	78.37	-2.194	-0.661	-2.856	38.73	-0.739		-0.824	16.10	-0.143	0.033	-0.110
92G	20.61	-0.512	-0.435	-0.947	-	-	-	-	21.04	-0.156	-0.330	-0.486
93A	24.26	-0.853	-0.440	-1.293	33.71	-0.540	-	-0.609	18.03	-0.317	-0.396	-0.712
94L	24.38	-1.424	-	-1.435	18.76	-0.642	-0.143	-0.785	-	-	-	-
96K	-	-	-	-	36.13	1.917	-4.604	-2.687	-	-	-	-
98Q	43.76	0.439		0.217	15.58	0.494	-0.150	0.344	-	-	-	-

Abbreviations in the table are to be read as follows: Res - Residue; IASA - interface accessible surface area; desol - desolvation energy; ele - electric energy; bind - binding free energy.

Table 3
Pairwise decomposition of binding Free energy for some hotspot residues in Trx complexes

Trx res	T7pol-Trx			TrxR-Trx			Bt-Trx		
	T7polres	ΔE	ΔG_{bind}	TrxRres	ΔE	ΔG_{bind}	Btres	ΔE	ΔG_{bind}
W31	P267	n	-0.626	F141	n	-1.299	F380	n	-0.686
				C138	-0.528	-1.082	V178	n	-0.642
R73	E319	-1.460	-1.424	A237	-2.906	-2.520	A379	n	-0.574
	V329	-0.476	-0.845	R130	-1.698	-1.851	V179	-0.349	-0.760
I75				F142	-0.398	-1.299	E181	-0.731	-0.754
				G129	-0.827	-1.037	E70	-0.677	-0.674
				D213	-0.797	-0.797	D68	-0.624	-0.624
				G216	0.889	1.266	T180	-0.273	-0.530
	T327	-0.925	-1.466	C138	n	-0.833	V178	-0.752	-1.899
	V329	n	-0.822	F142	n	-0.800	F380	n	-0.552
	Y326	-0.403	-0.782				S177	-0.374	-0.511

Abbreviations in the table are to be read as follows: T7pol - T7 DNA polymerase; TrxR - *E.coli* Thioredoxin reductase; Bt - Bacterial tubulin (A chain), res - residues,

n - negligible; T7pol-Trx - T7 DNA polymerase thioredoxin complex; TrxR-Trx - Thioredoxin reductase Thioredoxin complex; Bt-Trx - bacterial tubulin Thioredoxin complex.

desolvation energy component of binding free energy in all three complexes. This indicates that these residues contribute to the affinity component of molecular recognition by thioredoxin. These residues occupy almost the central region of the binding surface of Trx. The charged residues Lys36, Glu44, Asp61, Tyr70, Arg73, Lys90 and Lys96 contribute either positively or negatively to the binding free energy only in the physiological complexes while they play no role in the non-specific Bt-Trx complex indicating that these residues may be involved in imparting specificity to the molecular recognition process of *E.coli* Trx. These charged residues border the binding surface of Trx and surround the region associated with high affinity and promiscuous binding. Similarly residues Gly33, Met37, Ile41, Pro64, Val91 and Leu94 contribute considerably to binding only in cases of specific complexes i.e. T7pol-Trx and TrxR-Trx. Residues in helix-3 Ala67 and Pro68 are found both in T7pol-Trx and Fnonspecific Bt-Trx complex and may be associated with promiscuous binding. The geometric arrangement of affinity determining regions or the hot spot region surrounded by a ring of energetically less important hydrophilic residues that protect the hot spots from attack of bulk solvent – is in line with the famous proposition of the O-ring theory. Figure 3 depicts the geometric organization of hot spot residues and other energetically important residues associated with specificity in the binding surface of Trx.

Interface cluster analysis was done to check whether energetically important residues are scattered across the interface or clustered together (Brinda et al., 2005). Interface cluster analysis was done for T7pol-Trx, TrxR-Trx and Bt-Trx complexes using $I_{\min} = 6\%$ and the results are shown in Table 4. The hydrogen bonded pair of Trp31 and Asp61 in thioredoxin is mainly involved in hydrophobic contacts with interface residues of target proteins. The long side chain of Arg73 in Trx contributes significantly to IASA and pairs with Val91 in T7pol-Trx complex and is involved in interface cluster formation mainly with aromatic polar residues (tyrosine) of T7polymerase. In TrxR-Trx complex it is involved in interface cluster formation with pocket residues Ser133, Asp139, F142 and Tyr143 of TrxR and

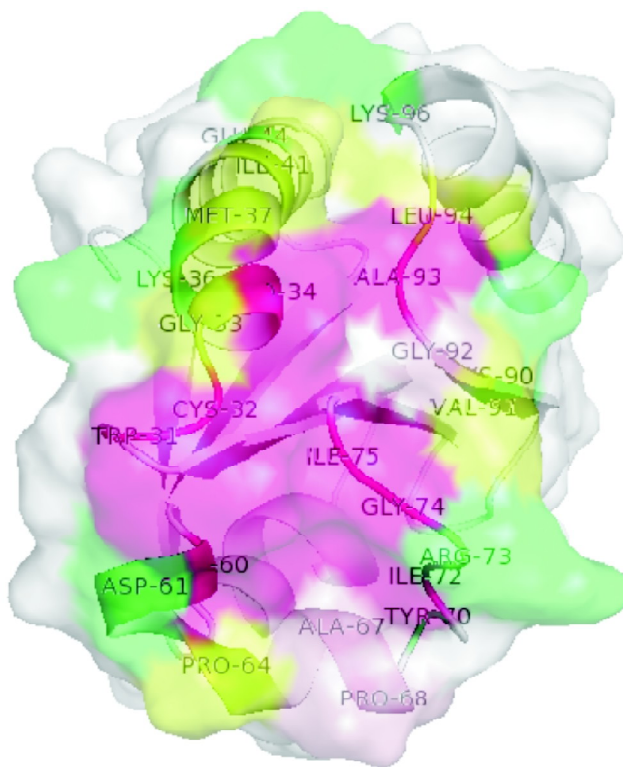


Figure 3: Molecular determinants of affinity and specificity. Regions associated with promiscuous binding are shaded in pink color. Regions associated with specificity are shown in green colour while other binding regions not involved in promiscuous binding are shown in yellow color

Table 4
Interface cluster analysis of Trx-target complexes

<i>Trx-T7P polymerase</i>	<i>Trx residues</i>	<i>T7 polymerase residues</i>
Cluster 1	R73, V91	Y320, Y326 and P328
Cluster 2	W31, D61	P267 and P287
Cluster 3	P68, I72	S263, Y265 and H331
Cluster 4	C32, I75	T327
TrxR-Trx	<i>Trx residues</i>	<i>Trx reductase residues</i>
Cluster 1	R73	S133, D139, F142 and Y143
Cluster 2	W31, D61	F141
Cluster 3	C32, I75	S135 and C138
Bt-Trx	<i>Trx residues</i>	<i>B tubulin residues</i>
Cluster 1	W31, D61	R396
Cluster 2	A67, P68, I72	T184, L393

contributes significantly to binding free energy. In the non-specific complex Bt-Trx it is not involved in interface cluster formation. This suggests that Arg73 may play a role in specificity of *E.coli* Trx. Thioredoxin residues Cys32 and Ile75 are involved in interface cluster formation with

polar residues of target proteins. Thioredoxin residues Pro68 and Ile72 are involved in interface cluster formation with polar residues of T7polymerase in T7pol-Trx complex while they form interface clusters with both polar and hydrophobic residues in the non-specific complex Bt-Trx. In TrxR-Trx complex they are not involved in interface cluster formation. This suggests that these residues may be involved in contribution to nonspecificity of Trx.

Conformational flexibility/ Structural plasticity of the binding surface

The snapshots generated from the 50ns MD trajectory of reduced Trx were subjected to RMSD based clustering using a cutoff of 2.0 Å and the overlay of representative snapshots from each cluster depicts the extent of conformational heterogeneity (Figure 4a). Regions around the N-terminal region of helix-2 and other loop residues across the binding surface particularly show extensive conformational flexibility. A detailed analysis of the time-dependent secondary structural changes analyzed using the DSSP program (Kabsch *et al.*, 1983) revealed that structure of the protruding helix-2 in reduced thioredoxin undergoes dynamical helix transitioning between a β_{10} helix and an α -helix with a coupled motion of the helix axis. Residues at the N- and C-termini of helix-2 (residues 33–38, 47, 48) are particularly vulnerable to this structural transition (Figure 4b).

During the MD simulations solvent accessible surface area of the protruding hydrophobic patch of reduced Trx comprising residues - Trp31, Cys32, Gly33 and Pro34 gets further solvent exposed leading to an increase in SASA by ~100 Å² (Figure 5a). Figure 5b compares two snapshots which have the lowest and highest SASA for this hydrophobic patch and demonstrates the adaptive nature of this hydrophobic patch. The boot shaped protrusion in snapshot B is due to complete exposure of this hydrophobic patch

Prokink (simulaid suite) analysis on the 10ns MD simulation trajectory of reduced thioredoxin shows that non-intact helices were found for 25% of the simulation time. The average bend angle from the simulations was found to be $37^\circ \pm 5.6^\circ$ and the average local helix tilt $4.06^\circ \pm 1.7^\circ$.

Essential Dynamics analysis performed on the whole equilibrated trajectory reveals that first ten eigenvectors are sufficient to describe more than 80% of the fluctuations. C^a atom based RMSF (Å²) for only the first ten eigenmodes has been calculated as they account for almost all the fluctuations. The motions along the top two eigen vectors clearly depict the protrusion of the active site helix-2 along with a coupled motion of the helix axis (Figure 6a). Low frequency modes 7, 10 and 11 from NMA analysis clearly reiterate the fact that there is a rotational and translational motion of the active site helix-2 as described in ED analysis (Figure 6b). In the high affinity complex of reduced Trx with T7 DNA polymerase the bound form of reduced Trx when superposed with unbound reduced Trx shows local helix tilt (~8 degrees) and translation as shown in Figure 6a. During the MD simulations it was observed that the N-terminal region of the helix rotates and translates towards the loop which precedes the C-terminal helix of the protein and in this process the cleft between the conserved hydrophobic patch adjoining the active site and the hydrophobic patch constituted by the conserved loop residues Gly⁹² and Ala⁹³ is sealed to form a contiguous surface (Figure 7).

The hydrophobic patch around the active site constituted by residues Trp31, Cys32, Gly33 and Pro34 contributes enormously to the desolvation free energy in all the analyzed thioredoxin complexes. Residues Ile75 and Val91 also contribute significantly to the desolvation free energy. Also residues Ile72 and Leu94 contribute to the desolvation free energy in obligate complexes such as Trx-T7 polymerase complex.

Changes in binding specificity of thioredoxin brought about by redox changes

Though the three dimensional structure of oxidized and reduced thioredoxin are strikingly similar only the reduced form of *E.coli* thioredoxin has been known to form tight complexes with T7 DNA polymerase and filamentous phage proteins (Huber *et al.*, 1987; Russel and Model 1986). Similarly mammalian Trx only in its reduced state forms inhibitory complexes with apoptosis signaling kinase (Saitoh *et al.*, 1998). To explain the observed binding differences between

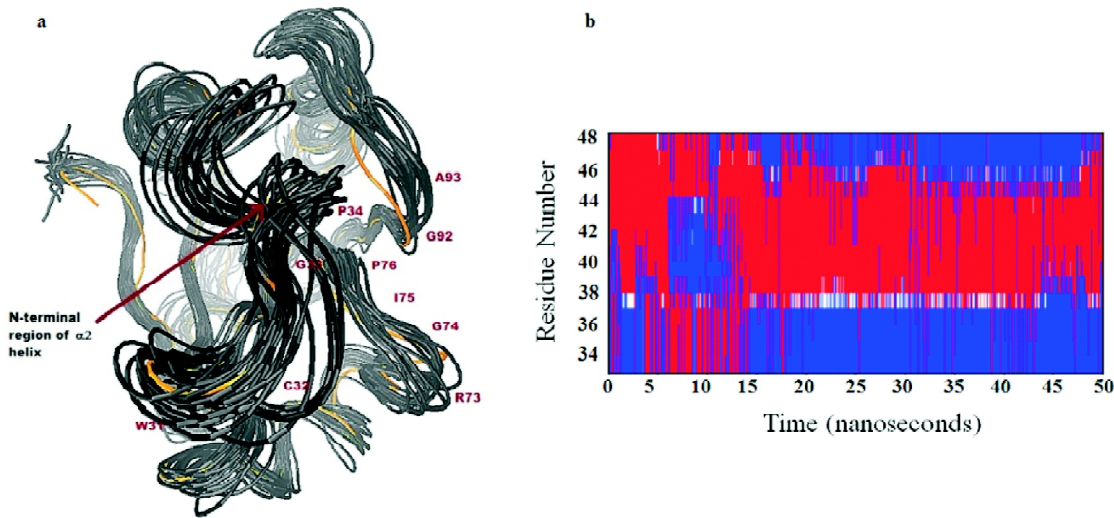


Figure 4: Conformational flexibility of *E. coli* thioredoxin.

- Overlay of snapshots of reduced thioredoxin generated by MD simulations showing the extent of conformational heterogeneity of the N-terminal region of helix-2 and other loop residues involved in binding. The conformer shown in orange tube representation corresponds to the NMR structure of free Trx and others shown in black tube representation correspond to MD generated structures of free Trx.
- Select portion of DSSP plot made using simulaid program showing helix transitioning of helix-2 (33-48) as function of time for the 50ns trajectory of reduced thioredoxin. α -helix is represented in blue while β_{10} helix is represented in red.

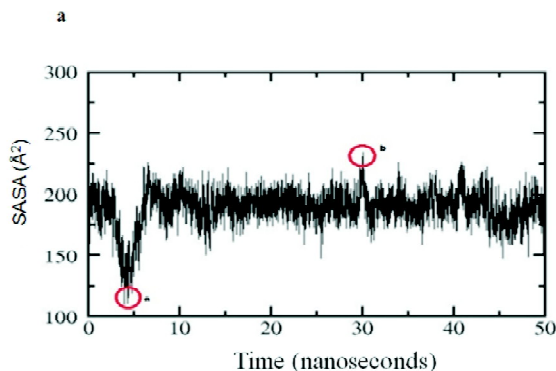


Figure 5: Protrusion of the active site binding surface.

- Solvent accessible surface area (SASA) profile for the 50ns length trajectory of the hydrophobic patch of the active site loop of *E. coli* thioredoxin. (Trp31, Cys32, Gly33 and Pro34).
- Surface representations of the snapshots having the lowest and highest SASA for the hydrophobic patch of the active site loop of *E. coli* thioredoxin (marked 'a' and 'b' respectively in the SASA plot). The binding surface has been shaded in orange. Note the foot shaped patch protruding out in snapshot b.

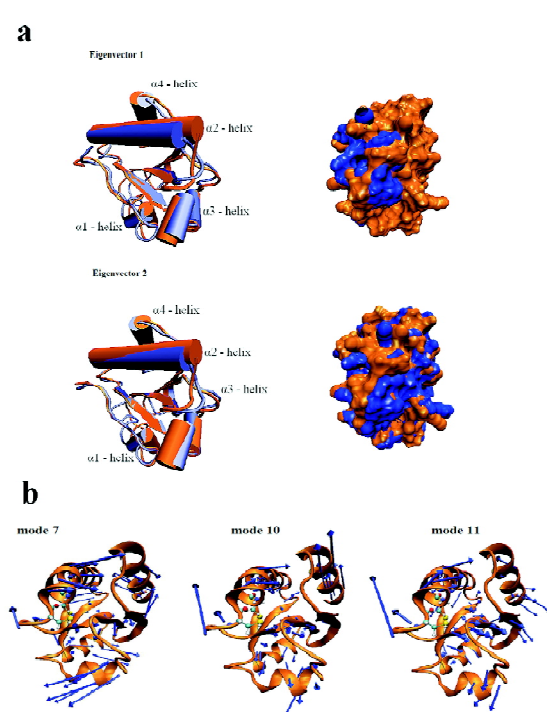


Figure 6: Motions of the protein along the top eigenmodes.

- Essential dynamics of the protein - Blue and brown represent the conformations for extreme values of PCA derived eigenvectors. Surface changes in the binding surface along the top two eigenmodes are also shown.
- Normal mode Analysis of the protein - Vector field representation of slow modes calculated by normal mode analysis of reduced thioredoxin which causes helix-2 tilt towards the loop which precedes helix-4. Only vectors having a length greater than the average atomic displacement for the mode considered are represented.

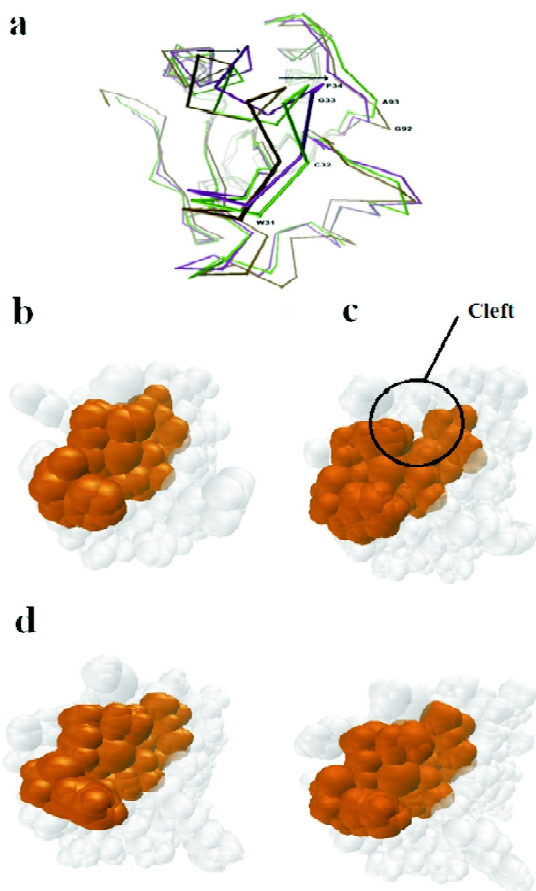


Figure 7: Conformational selection of bound state of Trx.

- Superposition of T7 polymerase bound rTrx, Thioredoxin reductase bound rTrx and unbound rTrx.
- T7 polymerase bound rTrx in Van der waals representation. The hydrophobic patch residues Trp31, Cys32, Gly33, Pro34, Pro76, Gly92 and Ala93 are shown in brown.
- Unbound rTrx in Van der waals representation. The hydrophobic patch residues Trp31, Cys32, Gly33, Pro34, Pro76, Gly92 and Ala93 are shown in brown.
- MD snapshots of unbound rTrx in Van der waals representation. The hydrophobic patch residues Trp31, Cys32, Gly33, Pro34, Pro76, Gly92 and Ala93 are shown in brown.

reduced Trx and oxidized Trx dynamical differences between the two forms of the protein have been probed. Figure 8 shows the RMSF and root mean square displacement along the top eigenmode from the ten nanoseconds MD trajectories for reduced Trx and oxidized Trx. The 5 \AA -strands which comprise the central β -sheet core of thioredoxin show strong correlation with one another. Strong correlation exists between the central β -sheet core and helix-3 and helix-4 (C-terminal helix). The central β -sheet core is strongly anti-correlated with helix-1 and helix-2.

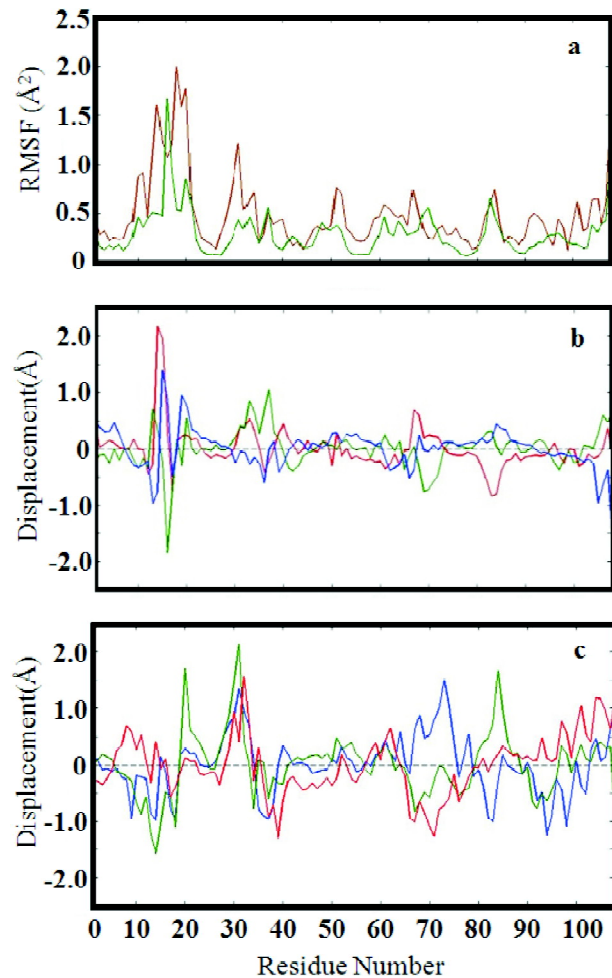


Figure 8: Dynamical differences between the reduced and oxidized forms of thioredoxin.

- Comparison of Residue wise C^a root mean square fluctuations (RMSF) in the reduced (brown) and oxidized (green) forms of the protein.
- Residue wise C^a root mean square displacements in the X, Y and Z directions for reduced thioredoxin.
- Residue wise C^a root mean square displacements in the X, Y and Z directions for oxidized thioredoxin.

Helix-2 (33 - 48) whose N-terminus harbours redox active disulphide/dithiol group is very strongly anti-correlated with the central β -sheet core. The helix-2 which is parallel to the β -sheet core slides away from it and protrudes the active site residues to the surface and forms a continuous stretch of binding surface with adjacent loop residues Gly92 and Ala93 (Figure 9). Absence of this predominant anticorrelated motion in oxidized Trx may explain the binding differences towards some target proteins for the two forms of Trx.

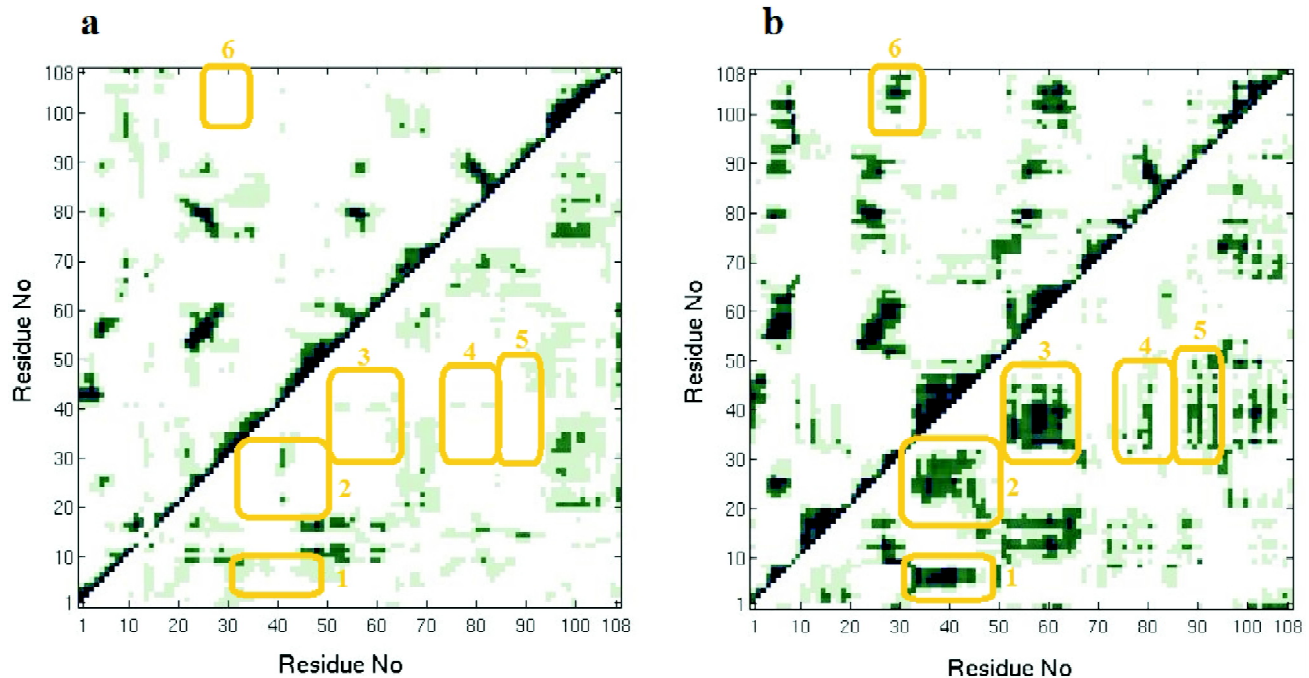


Figure 9: Dynamical Cross Correlation maps (DCCM) representing the collective atomic fluctuations for Oxidized thioredoxin (a) and reduced Thioredoxin (b). The very strong ($C_{ij} = \pm 0.85-1.0$), moderately strong ($C_{ij} = \pm 0.7-0.85$) and intermediate ($C_{ij} = \pm 0.5-0.7$) ones are represented by dark blue, dark green and pale green, respectively. The lower and upper triangles correspond to negative and positive correlations, respectively. Box 1 shows the anticorrelation of β -sheet 1 with helix-2, Box 2 shows the anticorrelation of β -sheet 2 with helix-2, Box-3 shows the anticorrelation of β -sheet 3 with helix-3, Box-4 shows the anticorrelation of β -sheet 4 with helix-2, Box-5 shows the anticorrelation of β -sheet 5 and adjoining loop residues with helix-2. Box-6 shows the correlation of C-terminal helix with the active site loop.

Discussion

From the interface analysis of the three different complexes it emerges that the binding surface of thioredoxin can be described as an adaptive, well exposed, non-polar and energetically important region on the surface of Trx that is primed for interaction with a variety of partner proteins. The usage of alternative hydrophobic contact points on the structurally plastic hydrophobic interaction surface may contribute considerably to the multispecificity of thioredoxin. The solvent exposed hydrophobic patch near the active site of thioredoxin exhibits transitions from an exposed to a buried closed state over a time scale of nanoseconds. Multispecific proteins have been known to use such hydrophobic interaction surface for the thermodynamic stabilization of protein-protein interactions (Fromer *et al.*, 2009). The geometric arrangement of affinity determining regions (hot spots) and specificity determining regions across the binding surface surrounded by a ring of energetically less important hydrophilic residues that protect the

hot spots from attack of bulk solvent – is in line with the famous proposition of the O-ring theory. The O-ring theory suggests that the hot spots are located at the core of the interface while the O-ring residues at its rim. Conformational flexibility has often been regarded as the most common reason for multi-specificity in protein-protein recognition (James and Tawfik, 2003). The region surrounding the binding site in thioredoxin undergoes conformational changes that are more pronounced compared with the whole molecule on average. Flexible proteins could easily adjust their structures to provide the most energetically favorable interactions with each of their interaction partners. Multispecific proteins have been shown to employ a wide range of conformational flexibility, to accommodate various target proteins, from reorientation of side-chains to mechanical motion of structural components with local alterations in secondary structure. The helix transitioning of the protruding helix-2 between α -helical and β_{10} helical forms in reduced thioredoxin contributes

to the structural plasticity associated with the active site binding surface. The increased structural plasticity of helix-2 in reduced thioredoxin may explain the binding affinity of reduced thioredoxin to a large number of diverse target proteins. Collective atomic motions form an essential part of protein functionality like catalysis and binding (Berendsen and Hayward, 2000). The essential dynamics method is ideal for separation of low frequency anharmonic motions from high frequency thermal fluctuations. The essential dynamics, as deduced from the 50ns MD simulation of thioredoxin, involves helix-2 rotation and translation accompanied by significant changes in the binding surface. The conformational changes upon binding have been found to occur usually along a few low energy modes of unbound proteins as the top ED modes with large amplitudes have significant projections on the direction of structural transitions between the bound and unbound forms of thioredoxin. Normal modes has been used to identify mobile regions of the protein and the direction of conformational change occurring during binding (Rios *et al.*, 2005). The first few low frequency normal modes describe well the direction of the observed conformational change associated with binding in accordance with the ED results. The central helix of calmodulin which is implicated in binding has been shown to undergo helix transitioning and bending (Van der Spoel *et al.*, 2006). Multispecific proteins having a broad range of binding may be expected to have rugged floors in their binding funnels (Tsai *et al.*, 1999). In agreement with the conformational selection model the conformational changes upon binding have been found to occur usually along a few low energy modes of unbound proteins calculated with NMA and MD approaches. The ED modes with large amplitudes have significant projections on the direction of structural transitions between the bound and unbound forms of thioredoxin.

Rugged floors represent substates whose energy barriers are low compared to the Boltzmann energy (K_{BT}) and thermal fluctuations can lead to significant population of more than one conformational state in solution. The ensemble generated using RMSD based clustering of snapshots from the 50ns MD simulation illustrates the extent of conformational

heterogeneity. The contribution of conformational heterogeneity to the observed multispecificity can be explained by invoking the conformational selection model which suggests that weakly populated, higher energy conformations are responsible for recognizing and binding to partners with subsequent population shift towards these conformers (Boehr and Wright 2008). Such intrinsic protein plasticity and reversible structural transition coupled to binding have been shown to work as regulatory switches to control certain biological processes (Tompa *et al.*, 2005).

Analysis of the consensus binding surface revealed that it was distinguished by a high degree of solvent accessibility and a predominantly non-polar character, suggesting that burial of exposed hydrophobic surface area is an important driving force behind binding at this site. The usage of alternative hydrophobic contact points on the structurally plastic hydrophobic interaction surface may contribute considerably to the multispecificity of Trx. Multispecific proteins have been known to use such hydrophobic interaction surface for the thermodynamic stabilization of protein-protein interactions (Fromer and Shifman *et al.*, 2009). The binding surface of Trx can be described as an adaptive, well exposed, non-polar and energetically important region on the surface of Trx that is primed for interaction with a variety of partner proteins.

Electrostatic interactions play an important role in determining the energetics of association and specificity of recognition in protein-protein interactions. Electrostatics may be vital to the development of mechanistic descriptions of protein - protein interactions. It has been shown in earlier studies that the electrostatic contributions from the nonbinding interfaces were able to control the orientation of protein binding interfaces in the process of protein-protein recognition (Han *et al.*, 2010). Long range electrostatic forces play a major role in the formation of the initial encounter complex with any of the electrostatically suitable partners. Charged residues Asp13, Lys52, Glu85 which are located on the nonbinding surface and opposite to the catalytic site of Trx have been shown to influence its interaction with its target 2-oxo acid

dehydrogenase (Bunik *et al.*, 2009). Interactions between charged and polar groups across the interface can be stabilizing, highly directional and distance dependent allowing the remarkable specificity that characterizes recognition process involving biological macromolecules. Directionality of electrostatic interactions imparts specificity in molecular recognition. In that study it also has been shown that alignment of dipoles plays a crucial role in successful complex formation (Eklund *et al.*, 1991). Intermolecular hydrogen bonds across the surface contribute to the interaction specificity of Trx with its target proteins.

Single interface hub proteins possess more than one hot spot in the binding surface and they employ alternate hot spots when binding to different target proteins. Geometric organization of the hotspot residues in Trx can place considerable restraints on the potential target proteins as shape complementarity plays a huge role in protein-protein interactions. It is generally observed that interfaces of hub proteins are enriched in flexible amino acids that can convey varying types of interactions. Small conformational changes at the side-chain level are frequently manifested in multi-specific binding. Protruding residues across the protein interface may coincide with anchoring residues in which case smooth recognition occurs without kinetically costly structural rearrangements. Once anchors are docked, an induced fit process further contributes to forming the final high-affinity complex. After protein-protein complexation imperfect indentations that remain unfilled are called as unfilled pockets while that disappear upon binding are called complemented pockets. Molecular recognition mechanisms may involve one of the interacting proteins to anchor a specific side-chain in a complemented pocket of the other protein to stabilize a near native bound intermediate (Rajamani *et al.*, 2004). Generally complemented pockets are rich in structurally conserved residues while unfilled pockets do not. Complemented pockets contain fewer amounts of hydrophilic residues than other surface pockets. The residue propensities for conserved residue types in complemented pockets include Trp, Gly, Pro, Cys, Tyr and Glu. In a study by Bogan and Thorn it has been shown that residues

in hotspots tend to overlap remarkably well with structurally conserved residues (Bogan *et al.*, 1998). Interface cluster analysis of the three Trx complexes reveals that the conserved residues form distinct localized clusters within the interface which enable the formation of a multispecific binding surface. The partner residue preferences for hot spots in Trx residues in all the complexes seem to be very similar.

Conformational change in thioredoxin can be associated with events such as disulfide bond formation or reduction, allowing one set of targets to bind in reduced state and another set of targets to bind in the oxidized state. RMSF plot clearly illustrates the dynamical differences between the two forms of the protein across the binding interface. Cross correlation analysis using DCCM maps clearly indicates vast differences in the collective dynamics between the two forms of the protein. The introduction of a disulfide bond seems to abolish the highly anticorrelated motions of the helices (I and II) with the beta sheet core of the protein. These anticorrelated motions may help in the helix-2 protrusion towards the binding partner. This combined with dynamic changes in the other binding regions of the protein makes reduced thioredoxin to adopt conformations with less planar binding surface for better protein-protein interactions. The overwhelming contribution of the first eigenvector from ED analysis arises from the fact that large scale conformational changes occurs, the main motion in this simulation being the displacement of helix-2 away from the body of the protein. This may help to expose the Cys32 to interact with residues in the binding partner and establish hydrogen bonds through SG to stabilize the interaction. In active site cysteine mutants the overall collective dynamics should be retained but substitution of Cys32 with other nonpolar aminoacids does not establish hydrogen bonds and therefore they have lowered affinity. But oxidized thioredoxin lacks the anticorrelated motion of the helix-2 and therefore completely lacks affinity for T7P and ASK-II proteins. The analysis of the dynamical properties of the two forms of thioredoxin highlights the differences in the global collective dynamics and structural plasticity at the binding region. These differences account for the selectivity of reduced thioredoxin in interactions

with T7P, ASK and proteins involved in filamentous phage growth. The impact of a single disulfide bond to alter the functional dynamics of this ubiquitous protein is quite surprising and may suggest new insights into the role of disulfide bridges as structural restraints and in influencing protein-protein interactions across the redox interactome.

Conclusions

Thioredoxin being the major disulfide reductase responsible for maintaining cytosolic proteins in their reduced state is central to the redox interactome. Thioredoxin is also involved in mechanical regulation of some target proteins through protein-protein interactions without the involvement of oxidoreductase activity. In this study the molecular features behind the multispecificity of thioredoxin to bind a wide range of proteins have been elucidated. Interplay of conformational selection and induced fit mechanisms enables thioredoxin to bind structurally diverse partner proteins. The conserved binding region of thioredoxin shows a lot of dynamic differences between the two redox forms of the protein accounting for their binding preferences.

Acknowledgements

MSSH would like to thank Prof.Siddhartha P.Sarma, MBU, IISc, for his valuable discussion during the manuscript preparation and Mr. Rajasekaran, MBU, IISc for help in use and troubleshooting of linux clusters. MSSH would like to acknowledge DBT and DST for funding the Computing facilities.

Abbreviations

Trx, Thioredoxin; PAPS, Phosphoadenylyl sulphate; DCCM, Dynamical cross correlation map; PCA, Principal Component Analysis; MD, Molecular Dynamics; SASA, Solvent accessible surface area; ED, Essential Dynamics; MM, Molecular mechanics; MM-PBSA, Molecular Mechanics Poisson Boltzmann Surface Area; IED, Interactive essential dynamics; RMSD, Root mean square deviation; RMSF, Root Mean Square Fluctuations; NMA, Normal Mode Analysis; T7pol, bacteriophage T7 DNA polymerase; TrxR, Thioredoxin reductase from *E.coli* ; BT, bacterial tubulin from Prosthecobacter dejongeii;

References

Arner, E.S.J. and Holmgren, A. (2000). Physiological functions of thioredoxin and thioredoxin reductase. *Eur. J. Biochem.* 267, 6102 - 6109.

- Berendsen, H.J.C. and Hayward, S. (2000). Collective protein dynamics in relation to function. *Curr. Opin. Struct. Biol.* 10, 165 - 169.
- Boehr, D.D. and Wright, P.E. (2008). How Do Proteins Interact? *Science*. 320, 1429 - 1430.
- Bogan, A.A. and Thorn, K.S. (1998). Anatomy of hot spots in protein interfaces. *J Mol Biol.* 280, 1 - 9.
- Brinda, K.V. and Vishveshwara, S. (2005). Oligomeric protein structure networks: insights into protein-protein interactions. *BMC Bioinformatics*. 6, 296 - 310.
- Bunik, V., Raddatz, G., Lemaire, S., Meyer, Y., Jacquot, J.P. and Bisswanger, H. (2009). Interaction of thioredoxins with target proteins: Role of particular structural elements and electrostatic properties of thioredoxins in their interplay with 2-oxoacid dehydrogenase complexes. *Prot. Sci.* 8, 65-74.
- Case, D.A., Darden, T.A., Cheatham, T.E., Simmerling, C.L., Wang, J., Duke, R.E., Luo, R., Merz, K.M., Pearlman, D.A., Crowley, M., Walker, R.C., Zhang, W., Wang, B., Hayik, S., Roitberg, A., Seabra, G., Wong, K.F., Paesani, F., Wu, X., Brozell, S., Tsui, V., Gohlke, H., Yang, L., Tan, C., Mongan, J., Hornak, V., Cui, G., Beroza, P., Mathews, D.H., Schafmeister, C., Ross, W.S. and Kollman, P.A (2006), AMBER 9, University of California, San Francisco.
- Doublie, S., Tabor, S., Long, A.M., Richardson, C.C. and Ellenberger, T. (1998). Crystal structure of a bacteriophage T7 DNA replication complex at 2.2 Å resolution. *Nature*. 391, 251 - 258.
- Eklund, H., Cambillau, C., Sjoberg, B.M., Holmgren, A., Jornvall, H., Hoog, J.O. and Branden, C.I. (1984). Conformational and functional similarities between glutaredoxin and thioredoxins. *EMBO J.* 3, 1443 - 1449.
- Eklund, H., Gleason, F.K. and Holmgren, A. (1991). Structural and functional relations among thioredoxins of different species. *Proteins: Struct., Funct., Genet.* 11, 13-28.
- Erijman, A., Aizner, Y. and Shifman, J.M. (2011). Multispecific recognition: Mechanism, Evolution, and Design. *Biochemistry*. 50, 602-611.
- Fromer, M. and Shifman, J.M. (2009). Tradeoff between stability and multispecificity in the design of promiscuous proteins. *PLoS Comput Biol.* 5, e1000627.
- Fujino, G., Noguchi, T., Takeda, K. and Ichijo, H. (2006). Thioredoxin and protein kinases in redox signaling. *Semin Cancer Biol.* 16, 427 - 435.
- Han, S., Yin, S., Yi, H., Mouhat, S., Qiu, S., Cao, Z., Sabatier, J.M., Wu, Y. and Li, W. (2010). Protein-Protein recognition control by modulating electrostatic Interactions. *J Proteome Res.* 9, 3118-3125.
- Hess, B., Kutzner, C., Van der Spoel, D. and Lindahl, E. (2008). GROMACS 4: Algorithms for Highly Efficient, Load-Balanced, and Scalable Molecular Simulation. *J. Chem. Theory Comp.* 4, 435-447.
- Huber, H.E., Tabor, S. and Richardson, C.C. (1987). Escherichia coli thioredoxin stabilizes complexes of bacteriophage T7 DNA polymerase and primed templates. *J. Biol. Chem.* 262, 16224 - 16232.

- Hunenberger, P.H., Mark, A.E. and Van Gunsteren, W.F. (1995). Fluctuation and Cross-correlation analysis of protein motions observed in nanosecond molecular dynamics simulations. *J. Mol. Biol.* 252, 492-503.
- James, L.C. and Tawfik, D.S. (2003). Conformational diversity and protein evolution - a 60-year-old hypothesis revisited. *Trends Biochem Sci.* 28, 361-368.
- Jeng, M.F., Campbell, A.P., Begley, T., Holmgren, A., Case, D.A., Wright, P.E. and Dyson, H.J. (1994). High-resolution solution structures of oxidized and reduced *Escherichia coli* thioredoxin. *Structure.* 2, 853 - 868.
- Jeong, H., Mason, S.P., Barabasi, A.L. and Oltvai, Z.N. (2001). Lethality and Centrality in protein networks. *Nature.* 411, 41- 42.
- Kabsch, W. and Sander, C. (1983). Dictionary of protein secondary structure: pattern recognition of hydrogen-bonded and geometrical features. *Biopolymers.* 22, 2577-2637.
- Karplus, M. and Kushick, J.N. (1981). Method for estimating the configurational entropy of macromolecules. *Macromolecules.* 14, 325-332.
- Kollman, P.A., Massova, I., Reyes, C., Kuhn, B., Huo, S., Chong, I., Lee, M., Lee, T., Duan, Y., Wang, W., Donini, O., Cieplak, P. and Srinivasan, J. (2000). Calculating Structures and Free Energies of Complex Molecules: Combining Molecular Mechanics and Continuum Models, *Acc. Chem. Res.* 33, 889-897.
- Kumar, J.K., Tabor, S. and Richardson, C.C. (2004). Proteomic analysis of thioredoxin targeted proteins in *Escherichia coli*. *Proc. Natl. Acad. Sci. USA.* 101, 3759 - 3764.
- Lennon, B.W., Williams Jr, C.H. and Ludwig, L.M. (2000). Twists in catalysis: Alternating conformations of *Escherichia coli* Thioredoxin reductase. *Science* 289, 1190 - 1194.
- Mezei, M. (2010). Simulaid: a simulation facilitator and analysis program. *J. Comp. Chem.*, 31, 2658-2668.
- Mongan, J. (2004). Interactive Essential Dynamics. *J Comput Aided Mol Des.* 18, 433-436.
- Raddtz, G., Kruft, V. and Bunik, V. (2000). Structural determinants for the efficient and specific interaction of thioredoxin with 2-Oxoacid dehydrogenase complexes, *Appl Biochem Biotechnol.* 88, 77 - 96.
- Rajamani, D., Thiel, S., Vajda, S. and Camacho, C.J. (2004). Anchor residues in protein-protein interactions. *Proc. Natl. Acad. Sci. USA.* 101, 11287-11292.
- Reynolds, C., Damerell, D. and Jones, S. (2009). ProtorP: a protein-protein interaction analysis server. *Bioinformatics* 25, 413-414.
- Rios, P.D.L., Cecconi, F., Pretre, A., Dietler, G., Michelin, O. and Piazza, F. (2005). Functional Dynamics of PDZ Binding Domains: A normal mode Analysis. *Biophys. J.* 89, 14-21.
- Russel, M. and Model, P. (1986). The role of thioredoxin in filamentous phage assembly. Construction, isolation and characterization of mutant thioredoxins. *J. Biol. Chem.* 261, 14997-15005.
- Saha, R.P., Bahadur, R.P., Pal, A., Mandal, S. and Chakrabarti, P. (2006). ProFace: a server for the analysis of the physicochemical features of protein-protein interfaces. *BMC Struct Biol.* 6, 11-16.
- Saitoh, M., Nishitoh, H., Fujii, M., Takeda, K., Tobiume, K., Sawada, Y., Kawabata, M., Miyazono, K. and Ichijo, H. (1998). Mammalian thioredoxin is a direct inhibitor of apoptosis signal-regulating kinase (ASK) 1. *EMBO J.* 17, 2596 - 2606.
- Schlieper, D., Oliva, M.A., Andreu, J.M. and Lowe, J. (2005). Structure of bacterial tubulin BtubA/B: Evidence for horizontal gene transfer. *Proc. Natl. Acad. Sci. USA.* 102, 9170 - 9175.
- Seeber, M., Cecchini, M., Rao, F., Settanni, G. and Caflisch, A. (2007). Wordom: a program for efficient analysis of molecular dynamics simulations. *Bioinformatics.* 23, 2625-7.
- Tompa, P., Szasz, C. and Buday, L. (2005). Structural disorder throws new light on moonlighting. *Trends Biochem Sci.* 30, 484-489.
- Tsai, C.J., Kumar, S., Ma, B. and Nussinov, R. (1999). Folding funnels, binding funnels, and protein function. *Protein Sci.* 8, 1181-1190.
- Tsai, C.J., Ma, B. and Nussinov, R. (2009). Protein-Protein interaction networks: how can a hub protein bind so many different partners. *Trends Biochem Sci.* 34, 594 - 600.
- Van der Spoel, D., De groot, B.L., Hayward, S., Berendsen, H.J.C. and Vogel, H.J. (1996). Bending of the calmodulin central helix: A theoretical study. *Protein Sci.* 5, 2044-2053.

